

Kinetics and Thermochemistry of the Reaction of 1-Chloroethyl Radical with Molecular Oxygen

Vadim D. Knyazev,* Ákos Bencsura,† Ilia A. Dubinsky,‡ and David Gutman§

Department of Chemistry, The Catholic University of America, Washington, D.C. 20064

Carl F. Melius

Combustion Research Facility, Sandia National Laboratory, Livermore, California 94551-0969

Selim M. Senkan*

Department of Chemical Engineering, University of California, Los Angeles, California 90024

Received: April 13, 1994; In Final Form: July 8, 1994[⊗]

The kinetics of the reaction $\text{CH}_3\text{CHCl} + \text{O}_2 \rightleftharpoons \text{CH}_3\text{CHClO}_2 \rightarrow \text{products}$ (1) has been studied at temperatures 296–839 K and He densities of $(3\text{--}49) \times 10^{16}$ molecule cm^{-3} by laser photolysis/photoionization mass spectrometry. Rate constants were determined in time-resolved experiments as a function of temperature and bath gas density. At low temperatures (298–400 K) the rate constants are in the falloff region under the conditions of the experiments. Relaxation to equilibrium in the addition step of the reaction was monitored within the temperature range 520–590 K. Equilibrium constants were determined as a function of temperature and used to obtain the enthalpy and entropy of the addition step of the reaction (1). At high temperatures (750–839 K) the reaction rate constant is independent of both pressure and temperature within the uncertainty of the experimental data and equal to $(1.2 \pm 0.4) \times 10^{-14}$ cm^3 molecule $^{-1}$ s $^{-1}$. Vinyl chloride ($\text{C}_2\text{H}_3\text{Cl}$) was detected as a major product of reaction 1 at $T = 800$ K. The rate constant of the reaction $\text{CH}_3\text{CHCl} + \text{Cl}_2 \rightarrow \text{products}$ (6) was determined at room temperature and He densities of $(9\text{--}36) \times 10^{16}$ molecule cm^{-3} using the same technique. The value obtained is $k_6 = (4.37 \pm 0.69) \times 10^{-12}$ cm^3 molecule $^{-1}$ s $^{-1}$. An estimate of the high-pressure limit for reaction 1 was determined using this measured k_6 and the k_1/k_6 ratio obtained by Kaiser et al.:¹ $k_1^\infty(T=298\text{K}) = (1.04 \pm 0.22) \times 10^{-11}$ cm^3 molecule $^{-1}$ s $^{-1}$. In a theoretical part of the study, structure, vibrational frequencies, and energies of nine conformations of $\text{CH}_3\text{CHClO}_2$ were calculated using ab initio UHF/6-31G* and MP2/6-31G** methods. The theoretical results are used to calculate the entropy change of the addition reaction $\Delta S^\circ_{298} = -152.3 \pm 3.3$ J mol $^{-1}$ K $^{-1}$. This entropy change combined with the experimentally determined equilibrium constants resulted in a $\text{CH}_3\text{CHCl}\text{--}\text{O}_2$ bond energy $\Delta H^\circ_{298} = -131.2 \pm 1.8$ kJ mol $^{-1}$. The room-temperature entropy ($S^\circ_{298} = 341.0 \pm 3.3$ J mol $^{-1}$ K $^{-1}$) and the heat of formation ($\Delta H^\circ_{f,298} = -54.7 \pm 3.7$ kJ mol $^{-1}$) of the $\text{CH}_3\text{CHClO}_2$ adduct were obtained.

Introduction

Due to the increasing usage of combustion as an effective treatment process for the disposal of hazardous organic wastes, including chlorinated hydrocarbons (CHC), kinetic modeling of the combustion of CHCs is a rapidly growing field of study. However, the success of such modeling is currently limited by a lack of fundamental knowledge about the mechanisms, specific pathways, and kinetic parameters of important elementary reactions, including the reactions of chlorinated alkyl radicals. The latter reactions are also important in the production of useful C_2 chemicals from natural gas by controlled pyrolysis and oxidative pyrolysis.^{2,3}

In the combustion processes, oxidation of polyatomic free radicals (R) by molecular oxygen is a key elementary step. The kinetics of the reactions of chlorine-containing alkyl radicals with O_2 has not been extensively studied, especially at high

temperatures. The addition process, which is the dominant reaction path at low temperatures, has been characterized for several C_1 chlorinated alkyl radicals (refs 4 and 5 and references therein). The results of studies of the temperature dependence of equilibrium in reactions $\text{R} + \text{O}_2 \rightleftharpoons \text{RO}_2$ provide information on the $\text{R}\text{--}\text{O}_2$ bond energy.^{6,7} Such studies have supplied the first measures of the thermal stability of these chlorinated RO_2 intermediates. The bond strengths were shown to decrease with increasing chlorination, changing from 136 kJ mol $^{-1}$ for the $\text{CH}_3 + \text{O}_2$ reaction to 83 kJ mol $^{-1}$ in the case of $\text{CCl}_3 + \text{O}_2$. Such a weakening of the $\text{R}\text{--}\text{O}_2$ bond caused by the chlorination of R is expected to result in a lowering of the characteristic temperatures at which the change of mechanism of the $\text{R} + \text{O}_2$ reaction occurs. This change of mechanism (caused by the thermal instability of RO_2 with respect to dissociation to $\text{R} + \text{O}_2$) is a transition from a low-temperature addition reaction to a high-temperature regime where equilibrium in the addition step is reversed and further rearrangement of adduct becomes a main reaction pathway.

The kinetics of C_2 -saturated chlorinated alkyl radicals with O_2 has not yet been studied. These reactions involve isomer-specific kinetics which makes the task more difficult. However, distinguishing between isomers is critical here because the rates

* On leave from the Central Research Institute for Chemistry, Hungarian Academy of Sciences, P.O. Box 17, H-1525 Budapest, Hungary.

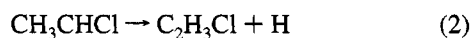
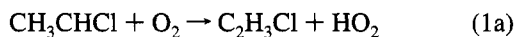
† Current address: Department of Chemistry, Massachusetts Institute of Technology, Cambridge, MA 02139.

‡ Deceased.

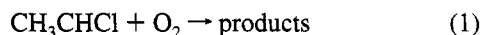
§ Abstract published in *Advance ACS Abstracts*, October 15, 1994.

and mechanisms of reactions of specific isomers may be substantially different.

A number of recent studies involving the kinetics of oxidation and pyrolysis of chlorinated hydrocarbons indicate the importance of the elementary reaction of the 1-chloroethyl radical with molecular oxygen.^{8,9} Chloroethyl radicals, CH_3CHCl and CH_2ClCH_2 , can be formed as a result of hydrogen abstraction from $\text{C}_2\text{H}_5\text{Cl}$ by OH, Cl, O, and H attack. It is important to note that CH_3CHCl radicals are preferentially produced due to the weaker $\alpha\text{-C-H}$ bond dissociation energies in $\text{C}_2\text{H}_5\text{Cl}$.^{9,10} During the pyrolysis and oxidative pyrolysis of such a relatively harmless compound as chloroethane, the formation of considerable amounts of vinyl chloride (a known human carcinogen) was observed^{8,11} and attributed⁹ to two elementary reactions:



Reaction 2 was experimentally confirmed as a source of vinyl chloride at high temperatures.¹² Although reaction 2 is the major reactive pathway for the CH_3CHCl radical during pyrolysis, in the presence of O_2 the reaction



effectively competes with the decomposition reaction.

Here we report the results of an experimental investigation of reaction 1 over a wide interval of temperatures and pressures. The distinctly different behavior of reaction 1 in the low (298–400 K), intermediate (520–590 K), and high (750–839 K) temperature regions is quantitatively characterized. Equilibrium constants of the addition step of reaction 1 were measured as a function of temperature, and the results were used to obtain the R-O_2 bond energy.

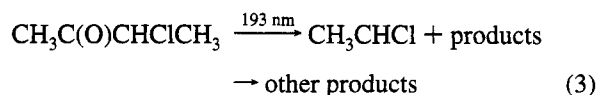
Experimental Section

1-Chloroethyl radicals were produced at elevated temperatures by pulsed laser photolysis, and their decay was subsequently monitored in time-resolved experiments using photoionization mass spectrometry. Details of the experimental apparatus¹³ used have been described before and so are only briefly reviewed here.

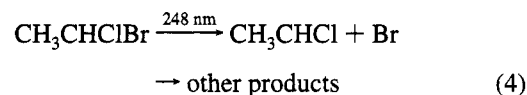
Pulsed unfocused 248- (or 193-) nm radiation (≈ 5 Hz) from a Lambda Physik EMG 201MSC excimer laser was directed along the axis of a heatable uncoated quartz or Pyrex reactor (1.05-cm i.d.). Gas flowing through the tube at ≈ 4 m s^{-1} contained the radical precursor (<0.5%), molecular oxygen in varying concentrations, and an inert carrier gas (He) in large excess. The flowing gas was completely replaced between laser pulses.

Gas was sampled through a hole (0.04- or 0.02-cm diameter) in the side of the reactor and formed into a beam by a conical skimmer before the gas entered the vacuum chamber containing the photoionization mass spectrometer. The reactor with the smaller sampling hole was used in the experiments that employed higher densities of the bath gas. As the gas beam traversed the ion source, a portion was photoionized and mass selected. 1-Chloroethyl radicals were ionized using the light from a chlorine resonance lamp (8.8–8.9 eV). Temporal ion signal profiles were recorded on a multichannel scaler from a short time before each laser pulse up to 20 ms following the pulse. Data from 3000 to 155 000 repetitions of the experiment were accumulated before the data were analyzed.

1-Chloroethyl radicals were produced by the pulsed, 193-nm laser photolysis of 3-chloro-2-butanone,



or by the 248-nm laser photolysis of 1-bromo-1-chloroethane,



The yield of 1-chloroethyl radicals from the photolysis of 3-chloro-2-butanone is sufficient for kinetic measurements only at relatively high temperatures, $T > 600$ K. Hence, the photolysis of 1-bromo-1-chloroethane was used as the source of CH_3CHCl radicals at low temperatures and both precursors were used at high temperatures, $750 \text{ K} \leq T \leq 839 \text{ K}$. At these conditions, neither the photolysis wavelength nor the nature of the radical precursor had any observable influence on the kinetics of 1-chloroethyl radical decomposition. Initial conditions (precursor concentration and laser intensity) were selected to provide low radical concentrations ($\leq 10^{11}$ molecule cm^{-3}) such that reactions between radical products had negligible rates compared to that of the reaction of 1-chloroethyl radicals with molecular oxygen.

A potentially complicating factor in these experiments is the possible isomerization of 1-chloroethyl radicals to 2-chloroethyl radicals during the photolysis process. We have studied the unimolecular decomposition of the 1-chloroethyl radical¹² over the temperature range 848–980 K. The onset of decomposition of CH_3CHCl at $[\text{He}] = 6 \times 10^{16}$ atom cm^{-3} occurs at approximately 800 K. The 2-chloroethyl radical is expected to decompose at significantly lower temperatures than does the 1-chloroethyl radical due to a C–Cl bond that is much weaker than the C–H bond. No signs of a possible contribution of this effect were detected in the current study or in the study of the unimolecular decomposition of CH_3CHCl ¹² in which the same photolytic sources of the 1-chloroethyl radical were used. Hence, the potential contribution of the 2-chloroethyl radical from photolysis of the precursors used in the current study can be neglected.

The gases used were obtained from Aldrich (3-chloro-2-butanone, 97%), Lancaster (1-bromo-1-chloroethane), and Matheson (He, >99.995%; O_2 , >99.6%). Precursors and oxygen were purified by vacuum distillation prior to use. Helium was used as provided.

Results

In the absence of molecular oxygen the kinetics of the 1-chloroethyl radical was that of an exponential decay with a first-order rate constant in the range 20–60 s^{-1} . This was attributed to the heterogeneous loss:



The reaction of CH_3CHCl with O_2 displayed distinctly different behavior in low (298–400 K), intermediate, and high (700–839 K) temperature intervals. It was possible to measure the bimolecular rate constants of reaction 1 as a function of temperature and pressure at 298 and 400 K in the low-temperature region and at 750 and 839 K in the high-temperature region. In the temperature range between 400 and 750 K the decay of 1-chloroethyl radicals in an excess of O_2 displayed nonexponential behavior which could be fit with a double-

TABLE 1: Conditions and Results of Experiments To Measure k_1 (T , [M])

| T (K) | [He] (10^{16} molecule cm^{-3}) | [precursor] (10^{13} molecule cm^{-3}) | [O ₂] (10^{13} molecule cm^{-3}) | k_1 (10^{-13} cm^3 molecule $^{-1}$ s $^{-1}$) | k_5 (s $^{-1}$) |
|---------|---|--|--|--|--------------------|
| 296 | 3.0 | 6.5 | 10.0–23.2 | 8.12 ± 1.13 | 30.4 |
| 298 | 6.0 | 2.7 | 3.1–15.7 | 12.8 ± 1.4 | 29.0 |
| 300 | 9.0 | 2.8 | 3.3–15.0 | 14.9 ± 2.1 | 31.9 |
| 298 | 12.0 | 4.7 | 3.3–12.4 | 18.1 ± 1.8 | 28.6 |
| 298 | 18.0 | 5.0 | 3.6–18.0 | 18.3 ± 1.9 | 32.2 |
| 299 | 24.0 | 3.7 | 3.7–13.7 | 20.4 ± 1.9 | 39.4 |
| 297 | 30.0 | 3.4 | 2.6–10.8 | 22.8 ± 2.8 | 39.0 |
| 299 | 36.0 | 3.5 | 1.8–10.4 | 23.8 ± 2.4 | 34.5 |
| 299 | 49.0 | 3.1 | 1.5–6.3 | 29.2 ± 4.7 | 37.6 |
| 400 | 3.0 | 1.1 | 7.6–35.3 | 2.91 ± 0.38 | 28.7 |
| 400 | 6.0 | 1.0 | 9.1–30.5 | 4.23 ± 0.49 | 23.2 |
| 400 | 4.5 | 1.1 | 7.9–32.0 | 3.52 ± 0.36 | 23.2 |
| 400 | 9.0 | 1.2 | 11.2–33.9 | 5.49 ± 0.52 | 22.3 |
| 400 | 12.0 | 1.4 | 9.9–28.0 | 6.44 ± 0.67 | 24.5 |
| 400 | 18.0 | 1.0 | 0.75–20.1 | 8.72 ± 0.96 | 46.4 |
| 400 | 18.0 | 1.1 | 5.0–20.9 | 9.76 ± 1.12 | 41.4 |
| 400 | 30.0 | 1.1 | 3.2–17.6 | 11.5 ± 1.2 | 47.8 |
| 400 | 42.0 | 1.1 | 2.3–17.5 | 13.6 ± 1.7 | 58.1 |
| 750 | 6.0 | 10.0 ^a | 2.3–12.2 | 0.161 ± 0.036 | 38.8 |
| 750 | 6.0 | 1.1 | 290–1150 | 0.085 ± 0.015 | 43.1 |
| 750 | 6.0 | 9.8 ^a | 300–1350 | 0.122 ± 0.027 | 40.9 |
| 750 | 18.0 | 1.2 | 544–1270 | 0.095 ± 0.020 | 31.0 |
| 839 | 6.0 | 7.8 ^a | 430–1710 | 0.119 ± 0.026 | 43.9 |
| 839 | 6.1 | 0.35 | 178–905 | 0.123 ± 0.019 | 26.5 |
| 839 | 18.2 | 0.25 | 375–1304 | 0.119 ± 0.026 | 54.7 |

^a 193-nm photolysis of 3-chloro-2-butanone was used for production of 1-chloroethyl radicals. 248-nm photolysis of CH₃CHClBr was used in all other experiments.

exponential function. Such behavior is indicative of an equilibrium in the reaction



It was possible to determine the equilibrium constants of the reaction 1b, -1b at $T = 520$ – 590 K (intermediate-temperature range) as a function of temperature.

Low (298–400 K) and High (750–839 K) Temperature Ranges. In the low- and high-temperature ranges the decay of CH₃CHCl in an excess of O₂ was exponential. The experiments were conducted under pseudo-first-order conditions with [O₂] in the range 7.5×10^{12} to 1.7×10^{16} molecule cm^{-3} . The 1-chloroethyl ion signal profiles were fit to an exponential function ($[\text{CH}_3\text{CHCl}]_t = [\text{CH}_3\text{CHCl}]_0 e^{-k't}$) by using a nonlinear least squares procedure. In a typical experiment to determine k_1 , the kinetics of the decay of CH₃CHCl radicals was recorded as a function of concentration of molecular oxygen. The values of k_1 were obtained from the slope of a linear plot of k' vs [O₂]. Experiments were performed to establish that the decay constants did not depend on the initial CH₃CHCl concentration (provided that the concentration was kept low enough to ensure that radical-radical reactions had negligible rates in comparison to the reaction with O₂), the concentration of the radical precursor or the laser intensity, the nature of the precursor, and the laser wavelength, 193 or 248 nm (in the high-temperature region, where both precursors were used). In the low-temperature range, rate constants of reaction 1 were determined at $T = 298$ K and [He] = $(3$ – $49) \times 10^{16}$ atom cm^{-3} and $T = 400$ K and [He] = $(3$ – $42) \times 10^{16}$ atom cm^{-3} . In the high-temperature region the k_1 values were measured at 750 and 839 K and [He] = $(6$ – $18) \times 10^{16}$ atom cm^{-3} . The conditions and results of these experiments are presented in Table 1. An example of a k' vs [O₂] plot is shown in Figure 1. The intercept at [O₂] = 0 corresponds to the rate of heterogeneous decay of CH₃CHCl radicals, k_5 .

The bimolecular rate constants, k_1 , exhibit pronounced falloff behavior at 298 and 400 K (Figure 2). The high-temperature

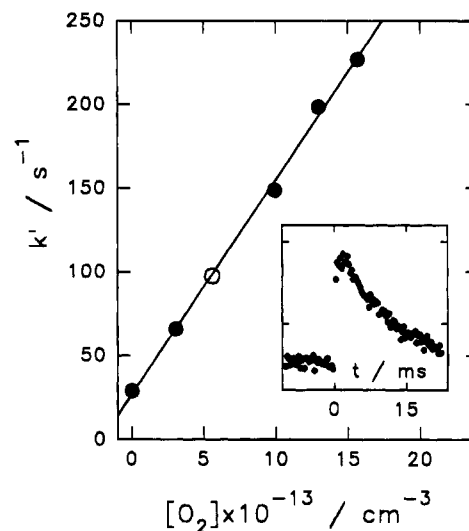


Figure 1. First-order CH₃CHCl decay rate k' vs [O₂]. The intercept at [O₂] = 0 corresponds to the rate of heterogeneous decay of CH₃CHCl radicals: $T = 298$ K, [He] = 6.0×10^{16} atom cm^{-3} , [CH₃CHClBr] = 2.7×10^{13} molecule cm^{-3} . The inset shows the recorded CH₃CHCl decay profile for the conditions of the open plotted point: [O₂] = 5.58×10^{13} molecule cm^{-3} , $k' = 97.5$ s $^{-1}$.

rate constant, however, appears to be independent of temperature and pressure within the experimental error limits under the conditions used (Table 1). Averaging of the experimental rate constants measured at $T = 750$ K and $T = 839$ K and [He] = $(3$ – $18) \times 10^{16}$ atom cm^{-3} results in the value of $k_1(T \geq 750\text{K}) = (1.2 \pm 0.4) \times 10^{-14}$ cm^3 molecule $^{-1}$ s $^{-1}$. Error limits here and throughout the text are 2σ unless otherwise noted.

An attempt was made to determine the products of reaction 1 at $T = 800$ K. The only molecular product of reaction 1 detected in the current study is vinyl chloride (detected using a hydrogen ionizing lamp with energy 10.2 eV). Although it was not possible to determine the branching ratio quantitatively, an estimate of the C₂H₃Cl yield relative to the amount of CH₃CHCl radicals consumed in reaction 1 of $\geq 50\%$ was made. The

TABLE 2: Conditions and Results of Experiments To Measure the Rate Constant Values (k_6) of the Reaction $\text{CH}_3\text{CHCl} + \text{Cl}_2$

| T (K) | [He] (10^{16} molecule cm^{-3}) | [CH_3CHClBr] (10^{13} molecule cm^{-3}) | [Cl_2] (10^{13} molecule cm^{-3}) | k_6 (10^{-13} cm^3 molecule s^{-1}) | k_5 (s^{-1}) |
|---------|---|---|--|--|---------------------------|
| 296 | 9.0 | 2.0 | 0.42–5.11 | 45.4 ± 5.4 | 54.9 |
| 296 | 18.0 | 8.9 | 1.10–4.20 | 41.9 ± 6.2 | 59.6 |
| 297 | 36.0 | 2.2 | 0.43–5.23 | 43.8 ± 5.9 | 60.2 |

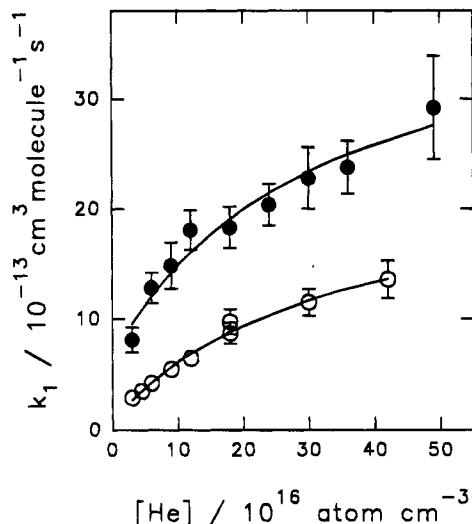


Figure 2. Falloff of the bimolecular rate constants k_1 at room temperature (filled circles) and 400 K (open circles). Lines through the data are the result of a parametric fit (see text).

sensitivity of the detection system to the concentration of $\text{C}_2\text{H}_3\text{Cl}$ was determined by adding a measured flow of vinyl chloride to the flow reactor. In the presence of molecular oxygen a yield of 80–120% of vinyl chloride relative to the change in the concentration of CH_3CHClBr (radical precursor) due to the initial photolysis was determined. This yield of $\text{C}_2\text{H}_3\text{Cl}$ was due to both reaction 1 and the production of vinyl chloride in the photolysis of CH_3CHClBr . Both of these sources of vinyl chloride were important. Photolysis of the precursor accounted for approximately 50–70% of the vinyl chloride produced, as estimated by comparing the signals of vinyl chloride in the presence and absence of molecular oxygen. This allows an estimate of 0.5 as the lower limit of the branching fraction to $\text{C}_2\text{H}_3\text{Cl}$ at 800 K.

High-Pressure Limit of Reaction 1 at Room Temperature. Reaction of CH_3CHCl Radicals with Cl_2 . The pressure range of the experimental apparatus did not allow us to extend the measurements of k_1 to He densities higher than 4.9×10^{17} atom cm^{-3} . Hence, the value of the high-pressure-limit rate constant of reaction 1 could not be measured directly.

In a recent study by Kaiser et al.¹ both reactions 1 and



were studied at $T = 298$ K and 700 Torr of air by UV photolysis/gas chromatography. The value of $k_6/k_1 = 0.42 \pm 0.06$ was obtained.

We studied reaction 6 at $T = 298$ K and $[\text{He}] = (9\text{--}36) \times 10^{16}$ atom cm^{-3} using the procedures described above. The concentrations of molecular chlorine employed were in the range $(4.2\text{--}52.3) \times 10^{12}$ molecule cm^{-3} , which ensured the pseudo-first-order decay of CH_3CHCl radicals. As expected, k_6 was independent of density within the above interval and equal to

$$k_6(T=298\text{K}) = (4.37 \pm 0.69) \times 10^{-12} \text{ cm}^3 \text{ molecule}^{-1} \text{ s}^{-1}$$

The conditions and results of the experiments to measure k_6 are presented in Table 2.

Using this value of k_6 , which we assume to be independent of pressure and thus to have the same value at 700 Torr (the pressure used in the experiments of Kaiser et al.), and the value of k_6/k_1 determined by Kaiser et al.,¹ we can calculate the value of the high-pressure-limit rate constant of reaction 1:

$$k_1^\infty(T=298\text{K}) = (1.04 \pm 0.22) \times 10^{-11} \text{ cm}^3 \text{ molecule}^{-1} \text{ s}^{-1}$$

Intermediate-Temperature Range. Determination of K_{eq} (T). In the temperature range between 400 and 750 K the decay of 1-chloroethyl radicals in the presence of O_2 displayed a nonexponential behavior, which could be fit with a double-exponential function. The kinetics of the CH_3CHCl decay was analyzed under the assumption that the following processes are important at these conditions: (1) heterogeneous loss of CH_3CHCl , reaction 5; (2) reversible addition of O_2 , reaction 1b,–1b, described by k_1 and k_{-1} ; (3) decay of the adduct, $\text{CH}_3\text{CHClO}_2$, due to heterogeneous loss and further reaction, which is described by a first-order rate constant k_d . The kinetics of the CH_3CHCl signal, $I(t)$, in such a system can be described by the following double-exponential expression:

$$I(t) = I_1 e^{-\lambda_1 t} + I_2 e^{-\lambda_2 t} \quad (I)$$

where

$$I_1 = I_0 \frac{k_1[\text{O}_2] + k_5 - \lambda_2}{\lambda_1 - \lambda_2}$$

$$I_2 = I_0 - I_1$$

$$\lambda_{1,2} = \frac{1}{2} (A \pm [A^2 - 4(k_{-1}k_5 + k_1[\text{O}_2]k_d + k_5k_d)]^{1/2})$$

$$A = k_1[\text{O}_2] + k_{-1} + k_5 + k_d$$

The values of k_5 were measured directly in the absence of O_2 . The temporal profile of the CH_3CHCl signal was fitted to formula I using k_1 , k_{eq} , I_0 , and k_d as adjustable parameters (here $K_{\text{eq}} = k_1/k_{-1}$ is the equilibrium constant of the reaction 1b,–1b, and I_0 is the signal value at $t = 0$). After the values of the above parameters were found, the fitting procedure was repeated several times with K_{eq} fixed at selected values in the vicinity of the best value, and the other three parameters floated. As a result, the sum of squares of deviation,

$$S = \sum (I_i(t) - I_{\text{calc}}(t))^2$$

was determined as a function of K_{eq} (with the three other parameters optimized) in the vicinity of its minimum and fitted with a parabolic function. From that information the experimental relative uncertainty ϵ of the fitted values of K_{eq} was determined using standard procedures.¹⁴ In each experiment to determine the values of K_{eq} , the data were accumulated until the criterion of $\epsilon \leq 10\%$ was satisfied. The equilibrium constants of reaction 1b,–1b were determined as a function of temperature from 520 to 590 K. The conditions and results of these experiments are presented in Table 3.

TABLE 3: Conditions and Results of Experiments To Measure the Equilibrium Constant of Reaction 1, -1

| <i>T</i> (K) | [CH ₃ CHClBr] (10 ¹³ molecule cm ⁻³) | [O ₂] (10 ¹⁴ molecule cm ⁻³) | <i>k</i> ₅ (s ⁻¹) | ln(<i>K</i> _p) ^a | - <i>f</i> | |
|------------------|---|--|--|--|------------|---------|
| | | | | | model 1 | model 2 |
| 520 | 1.06 | 7.48 | 25.1 | 11.788 ± 0.090 | 0.043 | 0.037 |
| 530 | 1.14 | 8.65 | 22.9 | 11.559 ± 0.038 | 0.047 | 0.043 |
| 530 | 0.994 | 9.09 | 25.5 | 11.447 ± 0.048 | 0.047 | 0.043 |
| 540 | 1.10 | 8.85 | 19.8 | 11.073 ± 0.053 | 0.052 | 0.047 |
| 540 | 1.21 | 4.21 | 18.9 | 11.177 ± 0.077 | 0.052 | 0.047 |
| 540 | 0.994 | 9.31 | 13.7 | 11.125 ± 0.066 | 0.052 | 0.047 |
| 540 | 1.14 | 18.1 | 24.2 | 10.859 ± 0.034 | 0.052 | 0.047 |
| 550 | 1.06 | 19.24 | 38.2 | 10.304 ± 0.055 | 0.058 | 0.049 |
| 550 | 1.07 | 18.5 | 35.0 | 10.592 ± 0.068 | 0.058 | 0.049 |
| 550 | 1.07 | 14.5 | 35.0 | 10.497 ± 0.081 | 0.058 | 0.049 |
| 550 | 1.06 | 14.3 | 21.3 | 10.329 ± 0.051 | 0.058 | 0.049 |
| 550 | 1.06 | 14.3 | 22.1 | 10.338 ± 0.072 | 0.058 | 0.049 |
| 560 | 1.06 | 23.0 | 36.2 | 9.888 ± 0.072 | 0.063 | 0.054 |
| 560 | 1.07 | 7.68 | 22.6 | 10.113 ± 0.086 | 0.063 | 0.054 |
| 560 ^b | 1.07 | 7.55 | 26.0 | 10.080 ± 0.078 | 0.063 | 0.054 |
| 560 | 0.436 | 7.59 | 26.6 | 10.070 ± 0.086 | 0.063 | 0.054 |
| 570 | 1.17 | 13.2 | 23.8 | 9.568 ± 0.028 | 0.068 | 0.059 |
| 570 | 1.10 | 9.32 | 27.8 | 9.543 ± 0.056 | 0.068 | 0.059 |
| 580 | 1.17 | 25.7 | 23.8 | 8.875 ± 0.031 | 0.075 | 0.065 |
| 580 | 1.17 | 16.7 | 25.8 | 9.148 ± 0.037 | 0.075 | 0.065 |
| 580 | 1.22 | 36.3 | 24.7 | 8.722 ± 0.045 | 0.075 | 0.065 |
| 590 | 1.17 | 35.4 | 20.4 | 8.436 ± 0.029 | 0.081 | 0.071 |
| 590 | 1.22 | 36.4 | 21.6 | 8.532 ± 0.074 | 0.081 | 0.071 |

^a Units of *K*_p are bar⁻¹. Error limits shown here are the values of the relative uncertainty ϵ in the *K*_{eq} values (see text). ^b This experiment was conducted with [He] = 6 × 10¹⁶ atom cm⁻³. [He] = 1.2 × 10¹⁷ atom cm⁻³ was used in all other experiments listed in this table.

The rate constant of the decay of the adduct, *k*_d, as mentioned above, is a sum of the rate constant of CH₃CHClO₂ heterogeneous loss and that of its further reaction to products other than CH₃CHCl + O₂. The fitted values of *k*₄ lie within the range 29–202 s⁻¹. Unfortunately, the potentially useful information on the CH₃CHClO₂ reaction to products cannot be separated from the rates of the wall reaction since it is impossible to measure the latter values independently.

Thermochemistry of Reaction 1b,-1b

The enthalpy change of reaction 1b,-1b at room temperature was obtained from the values of *K*_{eq}(*T*) using second law and third law analyses. The procedures used were described before.^{13,15,16} These calculations require knowledge of the temperature dependence of the thermodynamic functions (enthalpy and entropy) of CH₃CHCl and CH₃CHClO₂ which were obtained using the results of ab initio calculations.

Molecular Parameters of CH₃CHCl and CH₃CHClO₂. Molecular parameters of CH₃CHCl such as frequencies, rotational constants, and the barrier for internal rotation of the methyl group were taken from an ab initio study of Chen and Tschuikow-Roux.¹⁷ These authors optimized geometry and calculated harmonic frequencies at the UHF/6-31G* level of theory and calculated the barrier height for the CH₃ internal rotation at the MP2/6-311G** level. This barrier was found to be equal to 5.6 kJ mol⁻¹, but it reduced to 3.2 kJ mol⁻¹ if zero-point vibrational energy is included. We used the latter value in our model.

We studied the geometries and harmonic vibrational frequencies of CH₃CHClO₂ using the ab initio unrestricted HF method with the 6-31G* basis. A total of nine molecular conformations were investigated. Three of them represent stable configurations, and six represent saddle points corresponding to internal rotational barriers.

The most uncertain aspect of the structure and properties of the CH₃CHClO₂ adduct pertinent to the calculation of its entropy is the treatment of two hindered internal rotations: one rotation of the CH₃ group and one rotation of the O-O moiety about the C-O bond. The potential energy surface of the latter

torsional motion has three minima located (at the UHF/6-31G* level) at values of the CC-OO dihedral angle equal to 54.4, -162.7, and -78.8°. For each of these conformations of CH₃CHClO₂ a potential energy maximum for the methyl group rotation was found. The three saddle points corresponding to the potential energy maxima of the CC-OO rotation are found at 121.6, -101.1, and -14.2°. Harmonic vibrational frequencies of all of these nine conformations of the CH₃CHClO₂ adduct were calculated at the UHF/6-31G* level and scaled by a factor of 0.89. Energies were obtained at the MP2/6-31G** level. The optimized geometries, frequencies, and energies are listed in Tables 4–6. Reduced moments of inertia for internal rotations were calculated from the structural data by the method of Pitzer and Gwinn.^{18,19}

The potential energy surface of the CC-OO torsional motion has a complex form which cannot be easily approximated by any simple model. Among the three stable configurations (1–3 in Tables 4–6) structure 1 has the lowest energy, and structures 2 and 3 have energies 2.3 kJ mol⁻¹ higher than structure 1. Two of the three maxima represent relatively high rotational barriers (18.6 and 12.4 kJ mol⁻¹ for structures 4 and 6), while structure 5 has an energy of 3.7 kJ mol⁻¹, which is just 1.3 kJ mol⁻¹ above the nearest minimum, structure 3. The CC-OO dihedral angle of structure 5, -101.1°, is also close to that of structure 3, -78.8°. The resultant potential energy surface is more like a double well with one broad and one narrow minima. The potential energy surface of the CH₃ rotation, on the other hand, is a periodic triple well.

In order to estimate the degree of uncertainty in the entropy values of this torsional degree of freedom, we used two different models of the CH₃CHClO₂ adduct (Chart 1), both using an approximation of a sinusoidally hindered internal rotor. In model 1 the rotation about the C-O bond was assumed to have two minima and a barrier height of 15.5 kJ mol⁻¹ (the average of the energies of structures 4 and 6). In model 2 this rotation was treated as having three minima with the barrier height equal to 11.6 kJ mol⁻¹ (the average of structures 4, 5, and 6). In both models CH₃ rotors were treated as sinusoidally hindered with a barrier height of 16.3 kJ mol⁻¹ and symmetry number

TABLE 4: Interatomic Distances and Angles of the Nine Conformations of the CH₃CHClO₂ Adduct

| parameter ^a | conformation number | | | | | | | | |
|------------------------|---------------------|-------|--------|-------|--------|--------|--------|--------|--------|
| | 1 | 2 | 3 | 4 | 5 | 6 | 7 | 8 | 9 |
| C1-C2 | 1.511 | 1.513 | 1.511 | 1.513 | 1.511 | 1.512 | 1.527 | 1.530 | 1.529 |
| H5-C1 | 1.076 | 1.076 | 1.076 | 1.077 | 1.075 | 1.077 | 1.075 | 1.075 | 1.075 |
| H6-C2 | 1.082 | 1.082 | 1.082 | 1.082 | 1.082 | 1.082 | 1.082 | 1.081 | 1.082 |
| H7-C2 | 1.082 | 1.086 | 1.082 | 1.083 | 1.082 | 1.081 | 1.083 | 1.083 | 1.083 |
| H8-C2 | 1.084 | 1.085 | 1.084 | 1.084 | 1.085 | 1.081 | 1.080 | 1.080 | 1.080 |
| C14-C1 | 1.791 | 1.789 | 1.775 | 1.772 | 1.780 | 1.785 | 1.792 | 1.791 | 1.776 |
| O3-C1 | 1.401 | 1.405 | 1.420 | 1.429 | 1.416 | 1.421 | 1.403 | 1.406 | 1.421 |
| O9-O3 | 1.307 | 1.306 | 1.303 | 1.295 | 1.302 | 1.298 | 1.306 | 1.306 | 1.303 |
| C2-C1-H5 | 113.3 | 112.3 | 112.8 | 112.0 | 113.0 | 112.1 | 113.5 | 112.4 | 112.6 |
| C1-C2-H6 | 110.1 | 109.7 | 110.3 | 110.3 | 110.5 | 108.3 | 109.2 | 110.1 | 109.4 |
| C1-C2-H7 | 110.3 | 111.0 | 110.2 | 110.3 | 110.3 | 111.0 | 110.1 | 109.7 | 110.3 |
| C1-C2-H8 | 109.1 | 108.9 | 109.1 | 109.0 | 108.8 | 110.4 | 111.7 | 111.7 | 111.6 |
| C2-C1-C14 | 111.3 | 111.3 | 111.7 | 111.6 | 111.4 | 111.1 | 112.5 | 112.5 | 112.9 |
| C2-C1-O3 | 107.2 | 113.1 | 111.1 | 107.7 | 110.2 | 114.9 | 107.4 | 113.4 | 111.9 |
| C1-O3-O9 | 111.9 | 112.8 | 109.9 | 117.4 | 111.1 | 114.1 | 111.9 | 112.7 | 109.6 |
| H6-C2-C1-C14 | -59.3 | -61.5 | -61.8 | -61.2 | -60.8 | -57.7 | 121.4 | 119.4 | 119.1 |
| H7-C2-C1-C14 | 61.1 | 59.0 | 58.9 | 59.6 | 60.0 | 62.1 | -119.6 | -121.4 | -121.7 |
| H8-C2-C1-C14 | -179.2 | 179.3 | 178.8 | 179.2 | 179.6 | -176.9 | 1.2 | -1.1 | -1.0 |
| H6-C1-C2-H5 | 60.2 | 57.4 | 59.3 | 58.0 | 60.1 | 60.4 | -118.9 | -121.7 | -119.9 |
| H6-C2-C1-O3 | -179.6 | 173.8 | -179.2 | 173.6 | -179.1 | -177.4 | 0.8 | -5.6 | 1.2 |
| O9-O3-C1-C2 | -162.7 | 54.4 | -78.8 | 121.6 | -101.1 | -14.2 | -162.8 | 56.1 | -73.1 |

^a Parameters are X_i - Y_j distance between atoms X_i and Y_j (Å); X_i - Y_j - Z_k , angle between bonds X_i - Y_j and Y_j - Z_k (deg); X_i - Y_j - Z_k - W_n , dihedral angle determined by atoms X_i , Y_j , Z_k , and W_n (deg).

TABLE 5: Vibrational Frequencies^a of the Conformations of the CH₃CHClO₂ Adduct

| | vibrational frequencies (cm ⁻¹) | | | | | | | | | | | | | | | | | | |
|---|---|--|--|--|--|--|--|--|--|--|--|--|--|--|--|--|--|--|--|
| 1 | 2996, 2966, 2953, 2886, 1456, 1452, 1406, 1344, 1290, 1144, 1126, 1086, 999, 883, 661, 528, 422, 313, 278, 231, ^b 111 ^c | | | | | | | | | | | | | | | | | | |
| 2 | 3001, 2974, 2952, 2886, 1461, 1453, 1405, 1360, 1287, 1135, 1111, 1062, 988, 868, 689, 591, 382, 334, 272, 243, ^b 120 ^c | | | | | | | | | | | | | | | | | | |
| 3 | 2994, 2960, 2951, 2884, 1457, 1453, 1404, 1346, 1290, 1132, 1102, 1079, 1031, 870, 739, 445, 433, 304, 285, 246, ^b 78 ^c | | | | | | | | | | | | | | | | | | |
| 4 | 2983, 2959, 2949, 2883, 1455, 1453, 1403, 1341, 1311, 1171, 1092, 1073, 983, 870, 695, 540, 410, 314, 263, 248 ^b | | | | | | | | | | | | | | | | | | |
| 5 | 3006, 2962, 2947, 2881, 1455, 1453, 1404, 1346, 1287, 1150, 1105, 1078, 1020, 866, 736, 466, 398, 319, 298, 245 ^b | | | | | | | | | | | | | | | | | | |
| 6 | 2985, 2967, 2964, 2896, 1457, 1454, 1407, 1346, 1297, 1003, 841, 686, 559, 376, 332, 295, 271 ^b | | | | | | | | | | | | | | | | | | |
| 7 | 3000, 2978, 2954, 2893, 1461, 1456, 1414, 1343, 1287, 1134, 1124, 1073, 1016, 903, 667, 537, 429, 333, 281, 116 ^c | | | | | | | | | | | | | | | | | | |
| 8 | 3004, 2982, 2959, 2895, 1463, 1454, 1416, 1360, 1283, 1137, 1082, 1059, 1017, 869, 705, 609, 393, 354, 274, 139 ^c | | | | | | | | | | | | | | | | | | |
| 9 | 2995, 2972, 2954, 2892, 1461, 1454, 1413, 1344, 1289, 1128, 1104, 1060, 1036, 881, 748, 483, 435, 324, 277, 85 ^c | | | | | | | | | | | | | | | | | | |

^a Frequencies scaled by a factor of 0.89. ^b CH₃ torsion. ^c Torsional motion about the CC-OO bond.

TABLE 6: Energies of the Conformations of the CH₃CHClO₂ Adduct

| | $E(\text{UHF})^a$ (hartrees) | $E(\text{MP2})^b$ (hartrees) | ZPVE1 ^c (kJ mol ⁻¹) | ZPVE2 ^d (kJ mol ⁻¹) | $\Delta E(\text{UHF})^e$ (kJ mol ⁻¹) | $\Delta E(\text{MP2})^e$ (kJ mol ⁻¹) |
|---|------------------------------|------------------------------|--|--|--|--|
| 1 | -687.150 386 | -687.890 770 | 158.04 | 157.32 | 0 | 0 |
| 2 | -687.148 764 | -687.889 971 | 158.22 | 157.48 | 4.43 | 2.27 |
| 3 | -687.147 205 | -687.889 844 | 157.92 | 156.92 | 8.233 | 2.312 |
| 4 | -687.144 162 | -687.883 614 | 157.89 | | 16.19 | 18.64 |
| 5 | -687.146 966 | -687.889 379 | 158.04 | | 8.98 | 3.65 |
| 6 | -687.143 032 | -687.886 189 | 158.40 | | 19.67 | 12.39 |
| 7 | -687.144 242 | -687.884 786 | | 157.90 | 16.71 | 16.29 |
| 8 | -687.142 198 | -687.883 061 | | 158.19 | 17.95 | 18.85 |
| 9 | -687.140 553 | -687.882 852 | | 157.52 | 18.07 | 19.05 |

^a UHF energy with the 6-31G* basis. ^b MP2 energy with the 6-31G** basis. ^c Zero-point vibrational energy with the torsional rotation about the C-O bond excluded. ^d Zero-point vibrational energy with the torsional rotation of the CH₃ group excluded. ^e Energy differences between conformations with the appropriate ZPVE included. Conformations 2-6 relative to structure 1, ZPVE1 included; conformations 7, 8, and 9, relative to structures 1, 2, and 3, ZPVE2 included.

3. Thermodynamic functions of the hindered internal rotations under the approximations of models 1 and 2 were obtained from interpolation of the tables of Pitzer and Gwinn.¹⁷ The existence of two optical isomers of the CH₃CHClO₂ adduct was taken into account in the calculation of entropy.

Determination of ΔH°_{298} and ΔS°_{298} of Reaction 1b,-1b. The room-temperature enthalpy of reaction 1b,-1b was obtained from the data on $K_{\text{eq}}(T)$ using second law and third law analyses. First, the values of ΔG°_T of reaction 1b,-1b were obtained directly from the values of the equilibrium constant:

$$\ln(K_p/\text{bar}^{-1}) = -\Delta G^\circ_T/RT \quad (\text{II})$$

where K_p is the equilibrium constant in bar⁻¹.

The addition of a small "correction",

$$f(T) = \frac{\Delta H^\circ_T - \Delta H^\circ_{298}}{RT} - \frac{\Delta S^\circ_T - \Delta S^\circ_{298}}{R}$$

converts the right-hand side of II to a linear function of $1/T$ with the intercept at $1/T = 0$ equal to $\Delta S^\circ_{298}/R$ and the slope of the function equal to $-\Delta H^\circ_{298}/R$:

$$\ln(K_p) + f(T) = \frac{\Delta S^\circ_{298}}{R} - \frac{\Delta H^\circ_{298}}{RT}$$

The values of this "correction" function, $f(T)$ (less than 1% of $\ln(K_p)$), were calculated using the models of CH₃CHCl and CH₃-

CHART 1: Molecular Parameters of the Models of the CH₃CHClO₂ Adduct Used in the Thermochemical CalculationsVibrational Frequencies (cm⁻¹) for Models 1 and 2:

2996, 2966, 2953, 2886, 1456, 1452, 1406, 1344, 1290, 1144, 1126, 1086, 999, 883, 661, 528, 422, 313, 278.

Overall Rotations. Principal Moments of Inertia (amu Å²) for Models 1 and 2: $I_A = 97.54$; $I_B = 143.84$; $I_C = 226.309$ Internal Rotations. Reduced Moments of Inertia (amu Å²), Symmetry Numbers, and Rotational Barriers (kJ mol⁻¹):CH₃ rotation: $I_r = 3.08$; $\sigma = 3$; $V_0 = 16.3$ for Models 1 and 2

CC-OO rotation:

Model 1: $I_r = 11.45$; $\sigma = 1$; $V_0 = 15.5$; 2 minimaModel 2: $I_r = 11.45$; $\sigma = 1$; $V_0 = 11.6$; 3 minima

CHClO₂ radicals described above. The resultant values of $f(T)$ are listed in Table 3 for both models of CH₃CHClO₂.

In the second law treatment, both the enthalpy and entropy of reaction 1b, -1b were determined from the modified van't Hoff plot (Figure 3) of $(\ln(K_p) + f(T))$ vs $1/T$. The values of enthalpy (obtained from the slope of the plot) and entropy (obtained from the intercept) are

$$\Delta H^\circ_{298} = -131.6 \text{ (-131.4)} \pm 7.3 \text{ kJ mol}^{-1} \quad (\text{IIIa})$$

$$\Delta S^\circ_{298} = -152.9 \text{ (-152.4)} \pm 12.9 \text{ J mol}^{-1} \text{ K}^{-1} \quad (\text{IIIb})$$

The first of the values of ΔH°_{298} and ΔS°_{298} shown here were obtained using the "correction" function calculated with model 1 and the second values (in parentheses) with that for model 2. Error limits here and in other values of ΔH°_{298} and ΔS°_{298} are 2σ and include 6% experimental uncertainty in the concentration of O₂. The differences between the results obtained with models 1 and 2 are negligible in comparison with the experimental error limits.

In the third law treatment, the value of ΔS°_{298} of reaction 1b, -1b was calculated using the above models of the involved species:

$$\Delta S^\circ_{298} = -153.2 \text{ J mol}^{-1} \text{ K}^{-1} \text{ for model 1}$$

$$\Delta S^\circ_{298} = -151.5 \text{ J mol}^{-1} \text{ K}^{-1} \text{ for model 2}$$

The value of ΔH°_{298} was obtained from the slope of the line drawn through the experimental values of $\ln(K_p) + f(T)$ and the calculated intercept $\Delta S^\circ_{298}/R$ (Figure 3):

$$\Delta H^\circ_{298} = -131.7 \pm 0.3 \text{ J mol}^{-1} \text{ K}^{-1} \text{ for model 1}$$

$$\Delta H^\circ_{298} = -130.8 \pm 0.3 \text{ J mol}^{-1} \text{ K}^{-1} \text{ for model 2}$$

The results of the second law treatment and the third law treatment coincide. The error limits of the results of the third law treatment, however, are considerably lower than those of the second law treatment. We recommend using the average of the results of the third law treatment obtained with models 1 and 2 of the CH₃CHClO₂ adduct. A reasonable estimate of uncertainty of these thermodynamic functions is twice the differences in entropy and enthalpy between these two models:

$$\Delta H^\circ_{298} = -131.2 \pm 1.8 \text{ kJ mol}^{-1} \quad (\text{IVa})$$

$$\Delta S^\circ_{298} = -152.3 \pm 3.3 \text{ J mol}^{-1} \text{ K}^{-1} \quad (\text{IVb})$$

Discussion

This study provides the first experimental and theoretical investigation of the kinetics, thermochemistry, and products of reaction 1. The closest alkyl/O₂ system, the reaction of C₂H₅

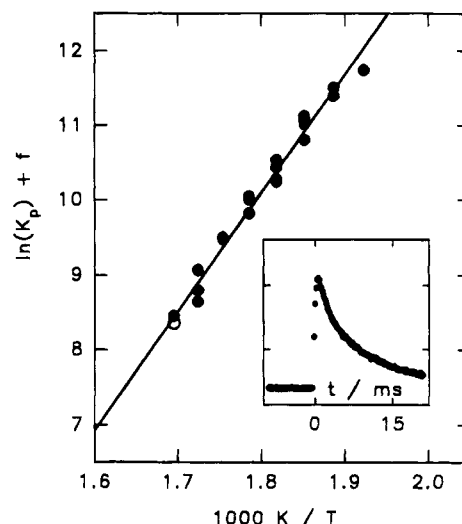


Figure 3. Modified van't Hoff plot of $(\ln(K_p) + f(T))$ vs $1000K/T$. The two lines corresponding to the second law and the third law treatments (see text) are indistinguishable on this plot. The inset shows the recorded CH₃CHCl decay profile for the conditions of the open plotted point: $T = 590 \text{ K}$, $[\text{O}_2] = 3.54 \times 10^{15} \text{ molecule cm}^{-3}$.

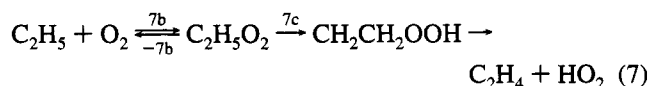
with molecular oxygen,



however, has received wide attention (refs 20–24 and references therein).

The most interesting and widely discussed part of the mechanism of reaction 7 concerns the reaction pathway at high temperatures, where the equilibrium in the addition process $\text{C}_2\text{H}_5 + \text{O}_2 \rightleftharpoons \text{C}_2\text{H}_5\text{O}_2$ is shifted to the left. While general agreement had been reached concerning the products of the high-temperature reaction ($\text{C}_2\text{H}_4 + \text{HO}_2$), uncertainty existed in the mechanism, i.e., whether these are the products of a direct abstraction reaction or a route involving the formation of an excited intermediate $\text{C}_2\text{H}_5\text{O}_2^*$ that undergoes further rearrangement to form $\text{CH}_2\text{CH}_2\text{OOH}$, which subsequently decomposes to $\text{C}_2\text{H}_4 + \text{HO}_2$.

The most recent combined experimental and theoretical study²¹ of reaction 7 decided in favor of the mechanism which proceeds through the formation of an excited adduct in the initial step of the reaction:



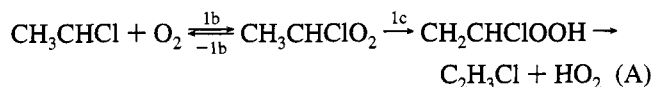
This excited adduct can undergo decomposition back to reactants (-7b), stabilization, or rearrangement (7c), which finally leads to $\text{C}_2\text{H}_4 + \text{HO}_2$.

Such a mechanism quantitatively explains all the experimental data available on reaction 7, including the low-temperature

kinetics (falloff in the bimolecular rate constant), equilibrium in the addition step (7b, -7b), high-temperature kinetics, and the product branching ratio as a function of temperature and pressure. It also predicts a 100% yield of the $C_2H_4 + HO_2$ channel due to the rearrangement (7c) of the unstabilized adduct in the low-pressure limit. The main argument that excludes the possible abstraction route is the absence of an apparent increase of the overall reaction rate constant with a temperature at $750\text{ K} \leq T \leq 1002\text{ K}$. Instead, a slight decrease or independence of temperature of the overall rate constant was observed. Wagner et al.²¹ suggested that the reaction pathway of excited $C_2H_5O_2$ leading to $C_2H_4 + HO_2$ proceeds via a five-membered ring transition state to form CH_2CH_2OOH , which subsequently decomposes. The rate-determining step is believed to be the hydrogen atom transfer. The barrier height for this hydrogen transfer proposed by Wagner et al. is 10 kJ mol^{-1} lower than the energy of reactants, $C_2H_5 + O_2$.

The latest ab initio study of this transition state by Quelch et al.,²⁴ although it did not confirm this value directly, suggested that, probably, the energy of the transition state is below that of the reactants. The energy of the transition state calculated by Quelch et al. was higher than the energy of reactants by 19 kJ mol^{-1} at the best level of theory used (CCSD(T)/DZP), but increasing the sophistication of the theoretical methods decreases the relative energy difference. This prompted the authors to suggest that such a trend should continue with further theoretical improvement.

Taking into account the similarity of the kinetics of reactions 1 and 7, we choose to interpret our results in terms of the following mechanism:



Here the hydrogen transfer reaction of 1c is the rate-determining step in the pathway leading to $C_2H_3Cl + HO_2$ products.

We do not include a possible direct abstraction path in this mechanism. This is supported by the fact that overall rate constants at high temperatures, when equilibrium in channels 1b, -1b is shifted toward reactants, show no apparent temperature dependence. The average values of the rate constant at $T = 750\text{ K}$ ($k_1 = 1.16 \times 10^{-14}\text{ cm}^3\text{ molecule}^{-1}\text{ s}^{-1}$) and $T = 839\text{ K}$ ($k_1 = 1.20 \times 10^{-14}\text{ cm}^3\text{ molecule}^{-1}\text{ s}^{-1}$) coincide. However, the very narrow temperature interval of the high-temperature study (750–839 K) and the scatter of the individual values (Table 1) do not allow us to exclude the possibility of some contribution from the abstraction reaction. Hence, a potential influence of such an abstraction route on the thermochemistry of reaction 1b, -1b needs to be assessed.

In order to determine the maximum effect of such an abstraction route on $\Delta H^\circ_{298}(1b, -1b)$, we need to estimate the upper limit of the abstraction rate constant (k_a) at the temperatures of the experiments in which the equilibrium constants were measured (520–590 K). We assume the value of $10^{-13}\text{ cm}^3\text{ molecule}^{-1}\text{ s}^{-1}$ as the lower limit for the preexponential factor of the abstraction reaction and obtain the upper limit of the abstraction rate constant at an average temperature of 795 K using the average high-temperature value, $k_1 = 1.2 \times 10^{-14}\text{ cm}^3\text{ molecule}^{-1}\text{ s}^{-1}$. This value together with the preexponential factor of 1×10^{-13} results in the lower limit of the abstraction activation energy $E_a = 14.1\text{ kJ mol}^{-1}$. Hence, the upper limit of the abstraction reaction rate constant at $T = 520\text{--}590\text{ K}$ is

$$k_a \leq 1 \times 10^{-13} \exp(-1700K/T) \text{ cm}^3 \text{ molecule}^{-1} \text{ s}^{-1} \quad (V)$$

Adding the $k_a[O_2]$ values resulting from formula V to k_5 in the treatment of the equilibrium measurements results in a reduction of K_{eq} values by an average of 7% with a maximum of 18% at the highest temperature (590 K). This change also affects the slope of the modified van't Hoff plot. The values of enthalpy of the addition step 1b, -1b recalculated assuming the maximum contribution of the abstraction reaction (formula II) are $\Delta H^\circ_{298} = -135.9 \pm 7.6\text{ kJ mol}^{-1}$ if the second law treatment is used with model 1 of the adduct and $\Delta H^\circ_{298} = -130.9\text{ kJ mol}^{-1}$ in the case of the third law treatment (average of models 1 and 2). The value of $\Delta S^\circ_{298} = -161.4 \pm 13.7\text{ J mol}^{-1}\text{ K}^{-1}$ is obtained in the case of the second law treatment. These changes in ΔH°_{298} and ΔS°_{298} introduced by the possible influence of an abstraction route in reaction 1 lie within the error limits of the formulas III and IV.

The chosen mechanism (A) of reaction 1 implies the existence of an intercept on a plot of the pressure dependence of the overall rate constant k_1 at low temperatures, similar to the case of reaction 7.²¹ This finite bimolecular reaction rate in the zero-pressure limit corresponds to reactive route 1c of the excited adduct CH_3CHClO_2 . We fitted the pressure-dependent k_1 values at 298 and 400 K with the modified Lindemann–Hinshelwood expression²⁵ with an additional pressure-independent component $k_1(P=0)$ included to account for the reaction rate in the zero-pressure limit. The value determined earlier, $k_1^\infty(T=298\text{K}) = 1.04 \times 10^{-11}\text{ cm}^3\text{ molecule}^{-1}\text{ s}^{-1}$, was used as k_1^∞ at both 298 and 400 K, assuming the approximate temperature independence of the high-pressure-limit addition rate constant by analogy²¹ with reaction 7. Three parameters were floated in the fitting procedure: $k_1(P=0)$, a third-order low-pressure rate constant, and F_{cent} . The experimental data are well reproduced by the above formalism. The resultant curves are shown in Figure 2 together with the experimental data. The scattering of the individual points and the limited pressure range of the experiments, however, result in a large uncertainty in the extrapolation to low pressures, which does not allow us to obtain meaningful values of the fitting parameters.

The weakening of the R–O₂ bond with the substitution of chlorine for hydrogen atoms on the carbon atom forming the C–O bond has been characterized for the case of $R = CH_3$.^{6,7} The bond strength (DH°_{298}) decreased from 136 kJ mol^{-1} in CH_3-O_2 ¹³ to 83 kJ mol^{-1} in CCl_3-O_2 ⁷ with intermediate values of 121 kJ mol^{-1} for CH_2Cl-O_2 and 106 kJ mol^{-1} for $CHCl_2-O_2$.⁶ This effect is consistent with the general weakening of the CH_3-X bond caused by the substitution of chlorine for hydrogen on the methyl group.²⁶ The current study provides the first example of the similar weakening of the R–O₂ bond for $R = C_2H_5$. The presence of the Cl atom in the $CH_3CHCl-O_2$ adduct reduces the R–O₂ bond energy by 11.5 kJ mol^{-1} (from 142.7 kJ mol^{-1} in the case of $C_2H_5-O_2$ ²¹ to 131.2 kJ mol^{-1} obtained in the current study).

We have determined the heat of formation of the CH_3CHClO_2 adduct using the enthalpy of reaction 1b, -1b (IV) and the newest and most directly determined value for the heat of formation of the CH_3CHCl radical reported by Seetula and Slagle.²⁷ These authors used their experimental activation energy of the reaction of CH_3CHCl radicals with HBr, the results of Miyokawa and Tschuikow-Roux²⁸ on the competitive bromination of C_2H_6 and C_2H_5Cl , and the experimental temperature dependence²⁹ of the rate constant of the reaction of Br atoms with C_2H_6 to obtain $\Delta H_f^\circ_{298}(CH_3CHCl) = 76.5 \pm 1.6(1\sigma)\text{ kJ mol}^{-1}$. This value is in perfect agreement with the "theoretical" value (76.4 kJ mol^{-1}) calculated by Chen and Tschuikow-Roux¹⁷ by coupling ab initio calculated energy changes for homodesmotic reactions with the known heats of formation of other reaction

components. Combining the value of Seetula and Slagle with that in expression IV, we obtain $\Delta H_f^\circ_{298}(\text{CH}_3\text{CHClO}_2) = -54.7 \pm 3.7 \text{ kJ mol}^{-1}$. The calculated entropy of the $\text{CH}_3\text{CHClO}_2$ adduct is $S^\circ_{298} = 341.0 \pm 3.3 \text{ J mol}^{-1} \text{ K}^{-1}$ (average of models 1 and 2; error limit is twice the difference between models 1 and 2).

Summary

The kinetics of the reaction



has been studied at temperatures $296 \text{ K} \leq T \leq 839 \text{ K}$ and He densities $(3-49) \times 10^{16} \text{ molecule cm}^{-3}$. Distinctly different kinetic behavior at low ($296 \text{ K} \leq T \leq 400 \text{ K}$), high ($750 \text{ K} \leq T \leq 839 \text{ K}$), and intermediate ($520 \text{ K} \leq T \leq 590 \text{ K}$) temperatures was investigated. Vinyl chloride ($\text{C}_2\text{H}_3\text{Cl}$) was detected as a major product of reaction 1 at $T = 800 \text{ K}$.

Equilibrium constants of reaction 1b,-1b were determined as a function of temperature over the range 520–590 K. In a theoretical part of the study, structure and vibrational frequencies of $\text{CH}_3\text{CHClO}_2$ were calculated. The results were used to calculate the entropy change of reaction 1b,-1b and, in combination with the experimental equilibrium data, to obtain the R–O₂ bond energy for reaction 1.

The rate constant of the reaction $\text{CH}_3\text{CHCl} + \text{Cl}_2$ was obtained at room temperature and densities $(3-36) \times 10^{16} \text{ molecule cm}^{-3}$.

Acknowledgment. This research was supported by the National Science Foundation, Division of Chemical, Biochemical and Thermal Engineering under Grant CTS-9311848. We also thank Professor Irene R. Slagle for her support of this work.

References and Notes

(1) Kaiser, E. W.; Rimai, L.; Schwab, E.; Lim, E. C. *J. Phys. Chem.* **1992**, *96*, 303.

- (2) Weissman, M.; Benson, S. W. *Int. J. Chem. Kinet.* **1984**, *16*, 307.
 (3) Senkan, S. M. *Chem. Eng. Prog.* **1987**, *12*, 58.
 (4) Fenter, F. F.; Lightfoot, P. D.; Caralp, F.; Lesclaux, R.; Niiranen, J. T.; Gutman, D. *J. Phys. Chem.* **1993**, *97*, 4695.
 (5) Fenter, F. F.; Lightfoot, P. D.; Niiranen, J. T.; Gutman, D. *J. Phys. Chem.* **1993**, *97*, 5313.
 (6) Russel, J. J.; Seetula, J. A.; Gutman, D.; Danis, F.; Caralp, F.; Lightfoot, P. D.; Lesclaux, R.; Melius, C. F.; Senkan, S. M. *J. Phys. Chem.* **1990**, *94*, 3277.
 (7) Russel, J. J.; Seetula, J. A.; Gutman, D.; Melius, C. F.; Senkan, S. M. *Symp. (Int.) Combust., [Proc.]* **1990**, *23*, 163.
 (8) Fisher, E. M.; Koshland, C. P.; Hall, M. J.; Sawyer, R. F.; Lucas, D. *Symp. (Int.) Combust., [Proc.]* **1990**, *23*, 895.
 (9) Senkan, S. M.; Yildirim, R.; Gutman, D. *Symp. (Int.) Combust., [Proc.]* **1992**, *24*, 749.
 (10) Niedzielski, J.; Tschuikow-Roux, E.; Yano, T. *Int. J. Chem. Kinet.* **1984**, *16*, 621.
 (11) Yildirim, R.; Senkan, S. M. *Ind. Eng. Chem. Res.* **1992**, *31*, 75.
 (12) Knyazev, V. D.; Bencsura, A.; Dubinsky, I. A.; Gutman, D.; Senkan, S. M. *Symp. (Int.) Combust., [Proc.]*, in press.
 (13) Slagle, I. R.; Gutman, D. *J. Am. Chem. Soc.* **1985**, *107*, 5342.
 (14) Bevington, P. R. *Data Reduction and Error Analysis for the Physical Sciences*; McGraw-Hill: New York, 1969.
 (15) Slagle, I. R.; Ratajczak, E.; Heaven, M. C.; Gutman, D.; Wagner, A. F. *J. Am. Chem. Soc.* **1985**, *107*, 1838.
 (16) Slagle, I. R.; Ratajczak, E.; Gutman, D. *J. Phys. Chem.* **1986**, *90*, 402.
 (17) Chen, Y.; Tschuikow-Roux, E. *J. Phys. Chem.* **1992**, *96*, 7266.
 (18) Pitzer, K. S.; Gwinn, W. D. *J. Chem. Phys.* **1942**, *10*, 428.
 (19) Pitzer, K. S. *J. Chem. Phys.* **1946**, *14*, 239.
 (20) Slagle, I. R.; Feng, Q.; Gutman, D. *J. Phys. Chem.* **1984**, *88*, 3648.
 (21) Wagner, A. F.; Slagle, I. R.; Sarzynski, D.; Gutman, D. *J. Phys. Chem.* **1990**, *94*, 1853.
 (22) Bozzelli, J. W.; Dean, A. M. *J. Phys. Chem.* **1990**, *94*, 3313.
 (23) Quelch, G. E.; Gallo, M. M.; Schaefer, H. F., III. *J. Am. Chem. Soc.* **1992**, *114*, 8239.
 (24) Quelch, G. E.; Gallo, M. M.; Schaefer, H. F., III.; Moncrieff, D. Submitted to *J. Am. Chem. Soc.*
 (25) Gilbert, R. G.; Luther, K.; Troe, J. *Ber. Bunsen-Ges. Phys. Chem.* **1983**, *87*, 169.
 (26) Weissman, M.; Benson, S. W. *J. Phys. Chem.* **1983**, *87*, 243.
 (27) Seetula, J. A.; Slagle, I. R. Manuscript in preparation.
 (28) Miyokawa, K.; Tschuikow-Roux, E. *J. Phys. Chem.* **1990**, *94*, 715.
 (29) Seakins, P. W.; Pilling, M. J.; Niiranen, J. T.; Gutman, D.; Krasnoperov, L. N. *J. Phys. Chem.* **1992**, *96*, 9847.